Molecular Vision 2019; 25:527-534 <http://www.molvis.org/molvis/v25/527>
Received 23 June 2019 | Accepted 19 September 2019 | Published 21 September 2019

Autosomal dominant nanophthalmos and high hyperopia associated with a C-terminal frameshift variant in *MYRF*

Owen M. Siggs,[1] Emmanuelle Souzeau,[1] James Breen,[2] Ayub Qassim,[1] Tiger Zhou,[1] Andrew Dubowsky,[3] Jonathan B. Ruddle,[4] Jamie E. Craig[1]

[1]Department of Ophthalmology, Flinders University, Bedford Park, South Australia, Australia; [2]South Australian Health and Medical Research Institute, Adelaide, South Australia, Australia; [3]SA Pathology, Flinders Medical Centre, Adelaide, Australia; [4]Department of Ophthalmology, University of Melbourne, Melbourne, Victoria, Australia

Purpose: Nanophthalmos is a rare subtype of microphthalmia associated with high hyperopia and an increased risk of angle-closure glaucoma. We investigated the genetic cause of nanophthalmos and high hyperopia in an autosomal dominant kindred.
Methods: A proband with short axial length, high hyperopia, and dextrocardia was subjected to exome sequencing. Human and rodent gene expression data sets were used to investigate the expression of relevant genes.
Results: We identified a segregating heterozygous frameshift variant at the 3′ end of the penultimate exon of *MYRF*. Using Myc-MYRF chromatin immunoprecipitation data from rat oligodendrocytes, *MYRF* was found to bind immediately upstream of the transcriptional start site of *Tmem98*, a gene that itself has been implicated in autosomal dominant nanophthalmos. *MYRF* and *TMEM98* were found to be expressed in the human retina, with a similar pattern of expression across several dissected human eye tissues.
Conclusions: C-terminal variants in *MYRF*, which are expected to escape nonsense-mediated decay, represent a rare cause of autosomal dominant nanophthalmos with or without dextrocardia or congenital diaphragmatic hernia.

Refractive error is the leading cause of visual impairment, and the second leading cause of blindness worldwide [1]. Precise developmental regulation of ocular axial length is essential to avoid refractive error, and the study of rare inherited refractive disorders has highlighted several critical genes and molecular pathways.

One of these rare disorders is nanophthalmos, characterized by high hyperopia associated with a reduction in posterior and anterior segment length, and a predisposition to primary angle-closure glaucoma [2,3]. Variants in at least four genes have been associated with nanophthalmos, with the majority due to recessive variants in membrane frizzled-related protein (*MFRP*; OMIM: 606227) [4] or protease, serine, 56 (*PRSS56*; OMIM: 613858) [5-7]. In rare cases, nanophthalmos may be inherited as a dominant trait, and we and others have reported two families segregating heterozygous missense variants in transmembrane protein 98 (*TMEM98;* OMIM: 615949) [8,9]. Common variants in *PRSS56* and *TMEM98* have also been implicated in multiple independent genome-wide association studies of myopia [10-12], highlighting the importance of studying nanophthalmos and other extremes of refractive error to understand the broader biology of common errors of refraction.

The latest gene to be implicated in nanophthalmos is myelin regulatory factor (*MYRF*; OMIM: 608329). The dominant *NNO1* locus (OMIM: 600165), initially mapped to chromosome 11 in a large family in 1998 [13], was recently found to harbor a C-terminal essential splice variant in *MYRF* [14], with simultaneous independent reports of other variants in nanophthalmos and high hyperopia [15,16]. We describe an additional family with dominant high hyperopia and nanophthalmos, and reveal a segregating heterozygous frameshift variant in *MYRF*.

METHODS

Human subjects: Patients and family members were recruited under the Australian and New Zealand Registry of Advanced Glaucoma [17]. Written informed consent was provided under protocols approved by the Southern Adelaide Clinical Human Research Ethics Committee (305–08), and adhering to the tenets of the Declaration of Helsinki.

DNA sequencing and analysis: DNA was prepared from whole blood and subjected to exome capture (Agilent SureSelect v5, Santa Clara, CA) as described [18]. DNA was prepared from venous blood samples, after temporary storage at -80°C, using the QIAGEN DNeasy Blood and Tissue Kit (Hilden, Germany), according to the manufacturer's instructions.

Correspondence to: Owen M Siggs, Department of Ophthalmology, Flinders University, Bedford Park, South Australia, Australia; Phone: +61 8 8204 5062; FAX: +61 8 8277 0899; email: owen.siggs@flinders.edu.au

Paired-end libraries were generated and sequenced on an Illumina NovaSeq 6000 (San Diego, CA) instrument, with reads aligned to the GRCh37 human reference, and variants were joint called across samples according to GATK Best Practice workflows. Variant annotation was performed using Variant Effector Predictor (VEP) [19], and annotated Variant Call Format (VCF) files packaged into Gemini databases for downstream analysis [20]. *MYRF* variant and exon coordinates refer to consensus transcript (NM_001127392.3) and protein (NP_001120864.1) sequences. Protein domains were as defined by UniProt (Q9Y2G1). Genomic Evolutionary Rate Profiling (GERP) constrained elements were defined by alignments across 35 mammalian species, and overlaid in Ensembl. *MYRF* variants were confirmed in a National Association of Testing Authorities (NATA)-accredited laboratory (SA Pathology, Flinders Medical Centre, Adelaide, Australia) using bidirectional capillary sequencing of the relevant PCR-amplified *MYRF* region. PCR products were sequenced and base called on an Applied Biosystems 3130xl Genetic Analyzer (ThermoFisher Scientific). PCR was performed using 100 ng of genomic DNA template in an AmpliTaq Gold reaction mix (Thermo Fisher Scientific, Waltham, MA). The following standard PCR conditions were used on a Veriti (Thermo Fisher Scientific) thermal cycler: Step 1, 95 °C for 10 min; Step 2, 95 °C for 30 s, 55 °C for 30 s, 72 °C for 1 min, repeated for 40 cycles; and Step 3, 72 °C for 7 min. PCR amplified products were prepared for sequencing with the ExoSAP method using 10 µl of each PCR reaction treated with 5 U of Exonuclease I (New England Biolabs, Ipswich, MA) and 1 U of Shrimp Alkaline Phosphatase (USB Corporation, Cleveland, OH) to remove residual primers and dNTPs. Bidirectional BigDye Terminator Cycle Sequencing (Thermo Fisher Scientific) reactions of the appropriate template and PCR primer were resolved and base called on an Applied Biosystems 3130xl Genetic Analyzer (Thermo Fisher Scientific). Detection of sequence variants was performed with the aid of Mutation Surveyor v4.0 (SoftGenetics LLC, State College, PA), with trace files assembled against the *MYRF* (NM_001127392.3) hg19 reference. The variant was deposited in ClinVar, with accession number VCV000635185.1.

Gene expression analysis: Expression of human *MYRF* (204073_s_at) and *TMEM98* (gnf1h00184_at) in selected tissues was retrieved from the GeneAtlas U133A data set [21]. Human cadaveric eye tissue dissection and RNA sequencing (RNA-seq) were performed as described [22]. Cadaveric human eyes with no known ocular disease were obtained from the Eye Bank of South Australia (Adelaide, Australia). Tissue dissection was performed under light microscope with a mean post-mortem time of 9.7 ± 5.3 h. Tissue from corneal epithelium, corneal stroma, corneal endothelium, trabecular meshwork (TM), pars plicata of the ciliary body, retina, optic nerve head, and optic nerve were collected and fixed in RNAlater solution (Thermo Fisher Scientific) for approximately 5 days prior to storage at -80 °C. A standard Trizol extraction protocol was used for RNA isolation (Thermo Fisher Scientific). RNA extracted from the pars plicata was passed through a Genomic-tip 20/G (QIAGEN, Hilden, Germany) as per the manufacturer's instructions to remove excess melanin. RNA quality was assessed using the Agilent Bioanalyzer 2100 RNA 6000 Nano Assay (Santa Clara, CA; mean RIN = 6.5 ± 1.8). A Qubit 2.0 Fluorometer (Thermo Fisher Scientific) was used to quantify RNA.

RESULTS

We ascertained a 35-year-old female proband of European ancestry with high hyperopia (+13.00 D), and short axial lengths (17.53 to 17.72 mm), who had previously undergone bilateral peripheral iridotomies for angle closure (Figure 1A). This trait appeared to segregate in a fully penetrant autosomal dominant manner across four generations (Figure 1A). The daughter of the proband (IV:1) had shallow anterior chambers (1.98 to 2 mm) with no visible angle structures and associated ocular hypertension (28 to 30 mmHg), for which she was treated with bilateral peripheral iridotomies. The proband's son (IV:2), had deep anterior chambers (3.67 to 3.7 mm) and no ocular hypertension. Examination of the proband's father (II:1) was remarkable for disc crowding. None of the affected family members had glaucoma at their most recent follow-up. Microcornea, papillomacular folds, uveal effusion syndrome, or marked vascular tortuosity was absent. The medical history of the index case (III:2) and her brother (III:3) was remarkable for dextrocardia, and although there were no reported genitourinary abnormalities, a routine chest X-ray in her affected son (IV:2) revealed an incidental right congenital diaphragmatic hernia (Figure 1B). The spectrum of the clinical details for all examined family members is summarized in Table 1.

Exome sequencing was performed on DNA from the proband, with no evidence of rare variants (gnomAD maximum allele frequency <0.01) predicted to be deleterious (Phred-scaled CADD score >10) in canonical transcripts of the previously known nanophthalmos genes (*TMEM98*, *PRSS56*, or *MFRP*). Given the phenotypic similarities of this case with a recently described family segregating an essential splice variant in *MYRF* [14], we searched for rare variants in the same gene. This revealed a heterozygous 1 bp deletion in *MYRF* (NM_001127392.3 c.3361delC), absent from gnomAD (v2.1.1), and predicted to introduce a C-terminal frameshift at codon 1121, followed by a premature termination codon

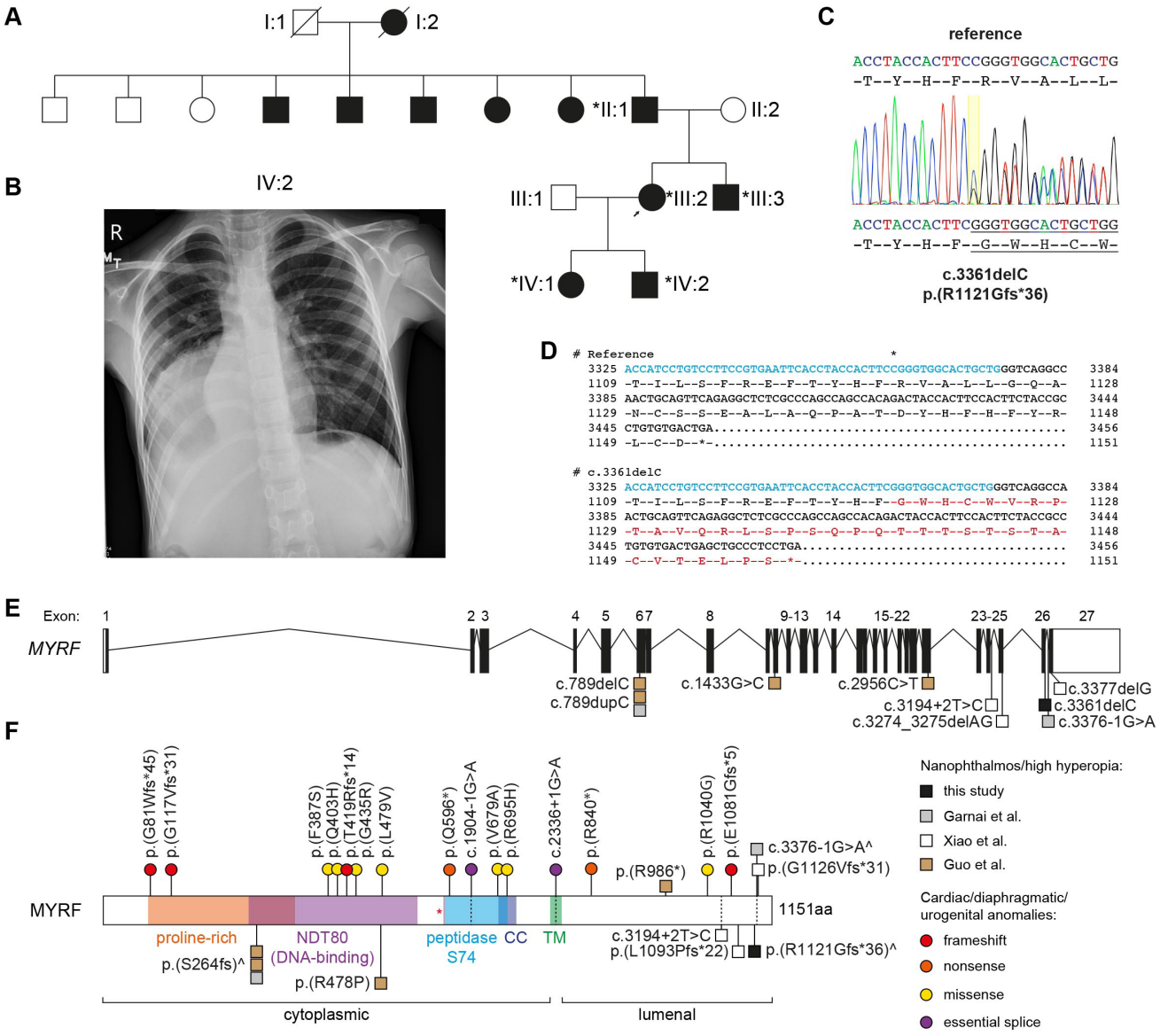

Figure 1. Autosomal dominant nanophthalmos and high hyperopia associated with a heterozygous frameshift variant in *MYRF*. **A**: Nanophthalmos pedigree showing affected (filled) and unaffected (unfilled) members. Asterisks indicate individuals in which the c.3361delC variant was confirmed with capillary sequencing. **B**: Chest X-ray of the proband's son (IV:2) showing a right congenital diaphragmatic hernia. **C**: Capillary sequencing trace of the *MYRF* c.3361delC variant in the proband (III:2), showing the reference and frameshifted variant sequences above and below the trace, respectively. **D**: Expanded cDNA and translated protein sequences from the *MYRF* reference sequence (NM_001127392.3), and the c.3361delC variant. Sequence encoded by the penultimate exon (exon 26) is highlighted in blue, with the frameshifted protein sequence highlighted in red. The c.3361 nucleotide is marked with an asterisk. **E**: *MYRF* locus schematic, showing the location of the variant described here (black symbol) and its proximity to variants described previously (gray [14] or white [15] symbols). **F**: MYRF protein schematic, showing the location of individual domains, and relative positions of reported disease-associated variants associated with nanophthalmos or high hyperopia (squares), or syndromic presentations (colored circles). Symbols (^) indicate nanophthalmos or high hyperopia variants associated with syndromic features. CC, coiled-coil domain; TM, transmembrane domain; red asterisk indicates the autolytic cleavage site.

Molecular Vision 2019; 25:527-534 <http://www.molvis.org/molvis/v25/527>

Table 1. Clinical parameters.

ID	Age	Gender	BCVA_RE	BCVA_LE	AL_RE (mm)	AL_LE (mm)	SE_RE (D)	SE_LE (D)	AC_RE (mm)	AC_LE (mm)	IOP_RE (mmHg)	IOP_LE (mmHg)	Intervention	Systemic
II:1	56	M	6/30	6/24	18.24	18.14	+10.75	+10.50	*3.98	*2.95	15	18	Phaco/IOL	.
III:2	36	F	6/24	6/9	17.50	17.69	+13.00	+13.00	2.91	2.85	12	10	PI BE	dextrocardia
III:3	33	M	.	.	.	.	.	.	.	.	.	.	.	dextrocardia
IV:1	8	F	6/15	6/7.5	17.88	18.05	+4.75	+4.00	2.00	1.98	28	30	PI BE	.
IV:2	9	M	6/6	6/38	18.40	18.19	+9.00	+10.00	3.70	3.67	13	14	Nil	CDH

Age represents age at recruitment. BCVA, best corrected visual acuity; AL, axial length; SE, spherical equivalent; AC, anterior chamber depth; IOP, intraocular pressure; RE, right eye; LE, left eye; BE, both eyes; CDH, congenital diaphragmatic hernia. In 8individual II:1, spherical equivalent values are before cataract surgery, with anterior chamber measurements (*) recorded after cataract surgery.

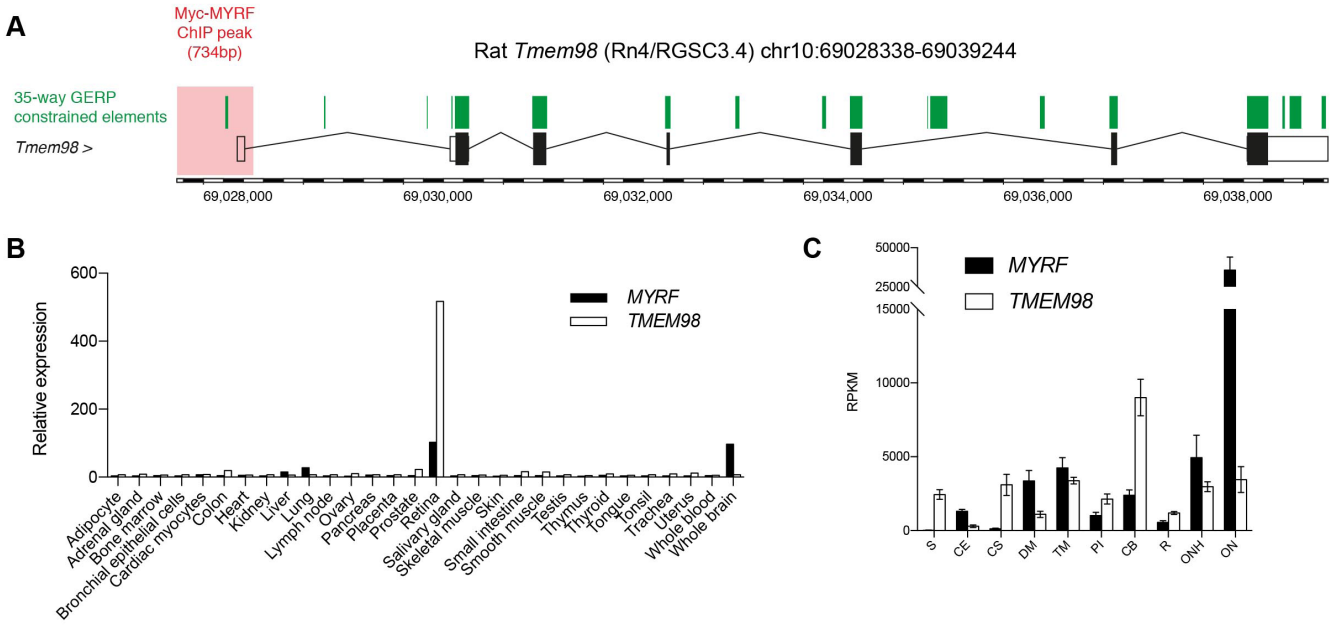

Figure 2. Coordinated expression of *MYRF* and *TMEM98* in human and rodent tissues. **A**: Myc-MYRF chromatin immunoprecipitation binding peak (highlighted in red) at the *Tmem98* locus in rat oligodendrocytes. Intervals constrained across 35 mammalian species are highlighted in green. **B**: Mean expression of *MYRF* and *TMEM98* in human tissue as measured with gene expression array [21]. **C**: Expression of *MYRF* and *TMEM98* transcripts in dissected human cadaveric eye tissue, represented as reads per kilobase per million mapped reads (RPKM). Bars represent mean with standard error of the mean (SEM; n=5–7 biologic replicates per tissue). S, sclera; CS, corneal stroma; CE, corneal epithelium; TM, trabecular meshwork; DM, Descemet's membrane; ON, optic nerve; ONH, optic nerve head; PI, peripheral iris; CB, ciliary body.

36 amino acids later in the terminal exon (NP_001120864.1 p.(Arg1121Glyfs*36); Figure 1C,D). This variant was validated with capillary sequencing in the proband (III:2), and all available affected family members (II:1, III:3, IV:1, and IV:2).

Compared to previously reported *MYRF* variants associated with congenital diaphragmatic hernia, congenital heart disease, and/or genitourinary abnormalities [23-27] (Figure 1E,F), the variant described here was at the 3′ end of the penultimate exon of *MYRF*, and therefore, may escape nonsense-mediated decay due to the introduction of a premature termination codon in the terminal exon (Figure 1D) [28]. The only described variants further downstream have been associated with isolated nanophthalmos and incompletely penetrant dextrocardia [14], or high hyperopia [15].

MYRF is translated as an endoplasmic reticulum (ER) membrane-bound protein, and following homotrimerization, is autoproteolytically cleaved to release an N-terminal transcriptional activator that translocates to the nucleus. One such transcriptional target is thought to be *TMEM98*, for which heterozygous variants have also been described to cause nanophthalmos [8,9]. Using a chromatin immunoprecipitation data set from rat oligodendrocytes probed with a Myc-MYRF construct [14], we identified a binding peak immediately upstream of and overlapping the *Tmem98* transcriptional start site, which also overlaps a genetic element constrained across 35 mammalian species (Figure 2A). *MYRF* and *TMEM98* were highly expressed in the human retina, with *MYRF* also highly expressed in the brain (Figure 2B). Within tissues of dissected cadaveric human eyes, *MYRF* and *TMEM98* shared an expression pattern more similar to one another than to *MFRP* and *PRSS56* (Figure 2C).

DISCUSSION

MYRF was initially described as a transcriptional regulator essential for oligodendrocyte differentiation and myelin gene expression [29]. Missense, nonsense, frameshift, and essential splice variants in *MYRF* have since been implicated in syndromic presentations of congenital diaphragmatic hernia, congenital heart disease, and genitourinary abnormalities [23-27]. For those with available mortality data, 2/6 died within the first month of life, with a third case electively terminated at 19 weeks' gestation [27]. At least one syndromic case also was associated with extreme hyperopia and short axial length [14], although it is unclear if detailed ocular examinations have been performed on other syndromic cases.

Similarly, it is unclear to what extent cardiac, diaphragmatic, and urogenital abnormalities have been investigated in individuals with apparently isolated nanophthalmos or hyperopia: Congenital diaphragmatic herniation was an incidental finding in at least one member of the kindred presented here.

The family presented here, along with others reported recently [14-16], represents a milder clinical presentation of *MYRF*-associated disease, with nanophthalmos or high hyperopia associated only occasionally with dextrocardia or congenital diaphragmatic hernia. There appear to be at least two important genetic distinctions between syndromic and non-syndromic *MYRF* variants. First, all syndromic *MYRF* variants reported thus far were found to be de novo, while at least three kindreds with nanophthalmos or high hyperopia show germline transmission of *MYRF* variants across multiple generations. Second, half (5/10) of the variants associated with nanophthalmos or high hyperopia occur in the final four exons of *MYRF*, or their associated splice sites. Three of these five affect either the terminal exon or the 3′ end of the penultimate exon, with a predicted termination codon introduced after read-through into the final intron. These three variants would, therefore, be expected to evade nonsense-mediated decay due to the 50 bp rule [28], and thus, be translated into protein with an altered C-terminus projecting into the ER lumen. The most C-terminal variant reported in a syndromic case to date is p.(Glu1081Glyfs*5), which lies in exon 25, and thus, expected to be degraded by nonsense-mediated decay [27]. Therefore, it would appear that more severe syndromic presentations are usually associated with *MYRF* haploinsufficiency, while isolated nanophthalmos may sometimes be a consequence of hypomorphic, dominant negative, or potentially hypermorphic variants that affect MYRF homotrimerization, autoproteolysis, or transcriptional activity.

Conspicuous exceptions to this include recently described variants in nanophthalmos [16], such as two independent frameshift variants affecting codon 264 (c.789delC, c.789dupC). One of these variants (NM_001127392.3, c.789dupC, p.(S264Qfs*74)) was also reported in a syndromic case of extreme axial hyperopia with mitral valve prolapse, unilateral cryptorchidism, and micropenis [14]. All three frameshift variants alter the length of an eight nucleotide cytosine mononucleotide repeat, and therefore, are a likely consequence of slipped-strand mispairing [30], but highlight that even N-terminal *MYRF* frameshift variants can lead to isolated nanophthalmos.

Variation in *MYRF* represents one of only two known genetic causes of autosomal dominant nanophthalmos. The second is *TMEM98*, first reported in a large European kindred [8]. *MYRF* encodes a membrane-bound transcription factor, which releases an active transcription factor complex after homotrimerization and autoproteolytic cleavage [31-33]. One of the transcriptional targets of this complex is *TMEM98*, and the TMEM98 protein itself binds directly to MYRF in the ER, where it acts as an inhibitor of MYRF autoproteolysis and nuclear translocation [34].

Studies in mice have suggested that variants in *TMEM98* associated with nanophthalmos represent gain-of-function alleles [35], which, in turn, would be predicted to increase inhibitory activity against MYRF. Although we cannot exclude the possibility of hypermorphic effects of certain *MYRF* alleles, reduced MYRF activity would be consistent with the predicted dominant-negative or loss-of-function effect of *MYRF* alleles suggested elsewhere [15,16], with similar support from the small eye phenotype of *myrf* knockdown zebrafish [15]. This intimate connection of two genes associated with nanophthalmos and high hyperopia provides further support for their roles in ocular development.

ACKNOWLEDGMENTS

Supported by the Australian National Health and Medical Research Council (NHMRC, Centres of Research Excellence Grant APP1116360 to JEC, Project Grant APP1107098 to JEC and OMS), and The Rebecca L Cooper Medical Research Foundation (Project Grant to OMS). JEC was an NHMRC Practitioner Fellow.

REFERENCES

1. Bourne RRA, Stevens GA, White RA, Smith JL, Flaxman SR, Price H, Jonas JB, Keeffe J, Leasher J, Naidoo K, Pesudovs K, Resnikoff S, Taylor HR. Vision Loss Expert Group. Causes of vision loss worldwide, 1990–2010: a systematic analysis. Lancet Glob Health 2013; 1:e339-49. .

2. Khan AO. Recognizing posterior microphthalmos. Ophthalmology 2006; 113:718-.

3. Khan AO. Posterior microphthalmos versus nanophthalmos. Ophthalmic Genet 2008; 29:189-.

4. Sundin OH, Leppert GS, Silva ED, Yang J-M, Dharmaraj S, Maumenee IH, Santos LC, Parsa CF, Traboulsi EI, Broman KW, Dibernardo C, Sunness JS, Toy J, Weinberg EM. Extreme hyperopia is the result of null mutations in MFRP, which encodes a Frizzled-related protein. Proc Natl Acad Sci USA 2005; 102:9553-8. .

5. Gal A, Rau I, El Matri L, Kreienkamp H-J, Fehr S, Baklouti K, Chouchane I, Li Y, Rehbein M, Fuchs J, Fledelius HC, Vilhelmsen K, Schorderet DF, Munier FL, Ostergaard E, Thompson DA, Rosenberg T. Autosomal-recessive posterior microphthalmos is caused by mutations in PRSS56, a gene

encoding a trypsin-like serine protease. Am J Hum Genet 2011; 88:382-90. .

6. Orr A, Dubé M-P, Zenteno JC, Jiang H, Asselin G, Evans SC, Caqueret A, Lakosha H, Letourneau L, Marcadier J, Matsuoka M, Macgillivray C, Nightingale M, Papillon-Cavanagh S, Perry S, Provost S, Ludman M, Guernsey DL, Samuels ME. Mutations in a novel serine protease PRSS56 in families with nanophthalmos. Mol Vis 2011; 17:1850-61. .

7. Nair KS, Hmani-Aifa M, Ali Z, Kearney AL, Ben Salem S, Macalinao DG, Cosma IM, Bouassida W, Hakim B, Benzina Z, Soto I, Söderkvist P, Howell GR, Smith RS, Ayadi H, John SWM. Alteration of the serine protease PRSS56 causes angle-closure glaucoma in mice and posterior microphthalmia in humans and mice. Nat Genet 2011; 43:579-84. .

8. Awadalla MS, Burdon KP, Souzeau E, Landers J, Hewitt AW, Sharma S, Craig JE. Mutation in TMEM98 in a large white kindred with autosomal dominant nanophthalmos linked to 17p12-q12. JAMA Ophthalmol 2014; 132:970-7. .

9. Khorram D, Choi M, Roos BR, Stone EM, Kopel T, Allen R, Alward WLM, Scheetz TE, Fingert JH. Novel TMEM98 mutations in pedigrees with autosomal dominant nanophthalmos. Mol Vis 2015; 21:1017-23. .

10. Verhoeven VJM, Hysi PG, Wojciechowski R, Fan Q, Guggenheim JA, Höhn R, MacGregor S, Hewitt AW, Nag A, Cheng C-Y, Yonova-Doing E, Zhou X, Ikram MK, Buitendijk GHS, McMahon G, Kemp JP, Pourcain BS, Simpson CL, Mäkelä K-M, Lehtimäki T, Kähönen M, Paterson AD, Hosseini SM, Wong HS, Xu L, Jonas JB, Pärssinen O, Wedenoja J, Yip SP, Ho DWH, Pang CP, Chen LJ, Burdon KP, Craig JE, Klein BEK, Klein R, Haller T, Metspalu A, Khor C-C, Tai E-S, Aung T, Vithana E, Tay W-T, Barathi VA. Consortium for Refractive Error and Myopia (CREAM), Chen P, Li R, Liao J, Zheng Y, Ong RT, Döring A, Diabetes Control and Complications Trial/Epidemiology of Diabetes Interventions and Complications (DCCT/EDIC) Research Group, Evans DM, Timpson NJ, Verkerk AJMH, Meitinger T, Raitakari O, Hawthorne F, Spector TD, Karssen LC, Pirastu M, Murgia F, Ang W, Wellcome Trust Case Control Consortium 2 (WTCCC2), Mishra A, Montgomery GW, Pennell CE, Cumberland PM, Cotlarciuc I, Mitchell P, Wang JJ, Schache M, Janmahasatian S, Janmahasathian S, Igo RP Jr, Lass JH, Chew E, Iyengar SK, Fuchs' Genetics Multi-Center Study Group, Gorgels TGMF, Rudan I, Hayward C, Wright AF, Polasek O, Vatavuk Z, Wilson JF, Fleck B, Zeller T, Mirshahi A, Müller C, Uitterlinden AG, Rivadeneira F, Vingerling JR, Hofman A, Oostra BA, Amin N, Bergen AAB, Teo Y-Y, Rahi JS, Vitart V, Williams C, Baird PN, Wong T-Y, Oexle K, Pfeiffer N, Mackey DA, Young TL, van Duijn CM, Saw S-M, Bailey-Wilson JE, Stambolian D, Klaver CC, Hammond CJ. Genome-wide meta-analyses of multiancestry cohorts identify multiple new susceptibility loci for refractive error and myopia. Nat Genet 2013; 45:314-8. .

11. Kiefer AK, Tung JY, Do CB, Hinds DA, Mountain JL, Francke U, Eriksson N. Genome-wide analysis points to roles for extracellular matrix remodeling, the visual cycle, and neuronal development in myopia. PLoS Genet 2013; 9:e1003299-.

12. Tedja MS, Wojciechowski R, Hysi PG, Eriksson N, Furlotte NA, Verhoeven VJM, Iglesias AI, Meester-Smoor MA, Tompson SW, Fan Q, Khawaja AP, Cheng C-Y, Höhn R, Yamashiro K, Wenocur A, Grazal C, Haller T, Metspalu A, Wedenoja J, Jonas JB, Wang YX, Xie J, Mitchell P, Foster PJ, Klein BEK, Klein R, Paterson AD, Hosseini SM, Shah RL, Williams C, Teo YY, Tham YC, Gupta P, Zhao W, Shi Y, Saw W-Y, Tai E-S, Sim XL, Huffman JE, Polašek O, Hayward C, Bencic G, Rudan I, Wilson JF. CREAM Consortium. 23andMe Research Team, UK Biobank Eye and Vision Consortium, Joshi PK, Tsujikawa A, Matsuda F, Whisenhunt KN, Zeller T, van der Spek PJ, Haak R, Meijers-Heijboer H, van Leeuwen EM, Iyengar SK, Lass JH, Hofman A, Rivadeneira F, Uitterlinden AG, Vingerling JR, Lehtimäki T, Raitakari OT, Biino G, Concas MP, Schwantes-An T-H, Igo RP Jr, Cuellar-Partida G, Martin NG, Craig JE, Gharahkhani P, Williams KM, Nag A, Rahi JS, Cumberland PM, Delcourt C, Bellenguez C, Ried JS, Bergen AA, Meitinger T, Gieger C, Wong TY, Hewitt AW, Mackey DA, Simpson CL, Pfeiffer N, Pärssinen O, Baird PN, Vitart V, Amin N, van Duijn CM, Bailey-Wilson JE, Young TL, Saw S-M, Stambolian D, MacGregor S, Guggenheim JA, Tung JY, Hammond CJ, Klaver CCW. Genome-wide association meta-analysis highlights light-induced signaling as a driver for refractive error. Nat Genet 2018; 50:834-48. .

13. Othman MI, Sullivan SA, Skuta GL, Cockrell DA, Stringham HM, Downs CA, Fornés A, Mick A, Boehnke M, Vollrath D, Richards JE. Autosomal dominant nanophthalmos (NNO1) with high hyperopia and angle-closure glaucoma maps to chromosome 11. Am J Hum Genet 1998; 63:1411-8. .

14. Garnai SJ, Brinkmeier ML, Emery B, Aleman TS, Pyle LC, Veleva-Rotse B, Sisk RA, Rozsa FW, Ozel AB, Li JZ, Moroi SE, Archer SM, Lin C-M, Sheskey S, Wiinikka-Buesser L, Eadie J, Urquhart JE, Black GCM, Othman MI, Boehnke M, Sullivan SA, Skuta GL, Pawar HS, Katz AE, Huryn LA, Hufnagel RB. Genomic Ascertainment Cohort, Camper SA, Richards JE, Prasov L. Variants in myelin regulatory factor (MYRF) cause autosomal dominant and syndromic nanophthalmos in humans and retinal degeneration in mice. PLoS Genet 2019; 15:e1008130-.

15. Xiao X, Sun W, Ouyang J, Li S, Jia X, Tan Z, Hejtmancik JF, Zhang Q. Novel truncation mutations in MYRF cause autosomal dominant high hyperopia mapped to 11p12-q13.3. Hum Genet 2019;138:1077-1090; .

16. Guo C, Zhao Z, Chen D, He S, Sun N, Li Z, Liu J, Zhang D, Zhang J, Li J, Zhang M, Ge J, Liu X, Zhang X, Fan Z. Detection of Clinically Relevant Genetic Variants in Chinese Patients With Nanophthalmos by Trio-Based Whole-Genome Sequencing Study. Invest Ophthalmol Vis Sci 2019; 60:2904-13. .

17. Souzeau E, Goldberg I, Healey PR, Mills RAD, Landers J, Graham SL, Grigg JRB, Usher B, Straga T, Crawford A, Casson RJ, Morgan WH, Ruddle JB, Coote MA, White A, Stewart J, Hewitt AW, Mackey DA, Burdon KP, Craig JE. Australian and New Zealand Registry of Advanced Glaucoma: methodology and recruitment. Clin Experiment Ophthalmol 2012; 40:569-75. .

18. Siggs OM, Souzeau E, Craig JE. Loss of ciliary zonule protein hydroxylation and lens stability as a predicted consequence of biallelic ASPH variation. Ophthalmic Genet 2019; 40:12-16. .

19. McLaren W, Gil L, Hunt SE, Riat HS, Ritchie GRS, Thormann A, Flicek P, Cunningham F. The Ensembl Variant Effect Predictor. Genome Biol 2016; 17:122-.

20. Paila U, Chapman BA, Kirchner R, Quinlan AR. GEMINI: integrative exploration of genetic variation and genome annotations. PLOS Comput Biol 2013; 9:e1003153-.

21. Su AI, Wiltshire T, Batalov S, Lapp H, Ching KA, Block D, Zhang J, Soden R, Hayakawa M, Kreiman G, Cooke MP, Walker JR, Hogenesch JB. A gene atlas of the mouse and human protein-encoding transcriptomes. Proc Natl Acad Sci USA 2004; 101:6062-7. .

22. Siggs OM, Souzeau E, Taranath D, Zhou T, Dubowsky A, Javadiyan S, Chappell A, Narita A, Elder J, Pater J, Ruddle J, Smith J, Kearns L, Staffieri S, Hewitt A, Mackey D, Burdon K, Craig JE. Congenital glaucoma with anterior segment dysgenesis in individuals with biallelic CPAMD8 variants [Internet]. bioRxiv. 2018. Available from: https://www.biorxiv.org/content/10.1101/297077v1

23. Pinz H, Pyle LC, Li D, Izumi K, Skraban C, Tarpinian J, Braddock SR, Telegrafi A, Monaghan KG, Zackai E, Bhoj EJ. De novo variants in Myelin regulatory factor (MYRF) as candidates of a new syndrome of cardiac and urogenital anomalies. Am J Med Genet A 2018; 176:969-72. .

24. Chitayat D, Shannon P, Uster T, Nezarati MM, Schnur RE, Bhoj EJ. An Additional Individual with a De Novo Variant in Myelin Regulatory Factor (MYRF) with Cardiac and Urogenital Anomalies: Further Proof of Causality: Comments on the article by Pinz et al. Am J Med Genet A 2018; 176:2041-3. .

25. Qi H, Yu L, Zhou X, Wynn J, Zhao H, Guo Y, Zhu N, Kitaygorodsky A, Hernan R, Aspelund G, Lim F-Y, Crombleholme T, Cusick R, Azarow K, Danko ME, Chung D, Warner BW, Mychaliska GB, Potoka D, Wagner AJ, ElFiky M, Wilson JM, Nickerson D, Bamshad M, High FA, Longoni M, Donahoe PK, Chung WK, Shen Y. De novo variants in congenital diaphragmatic hernia identify MYRF as a new syndrome and reveal genetic overlaps with other developmental disorders. PLoS Genet 2018; 14:e1007822-.

26. Hamanaka K, Takata A, Uchiyama Y, Miyatake S, Miyake N, Mitsuhashi S, Iwama K, Fujita A, Imagawa E, Alkanaq AN, Koshimizu E, Azuma Y, Nakashima M, Mizuguchi T, Saitsu H, Wada Y, Minami S, Katoh-Fukui Y, Masunaga Y, Fukami M, Hasegawa T, Ogata T, Matsumoto N. MYRF haploinsufficiency causes 46,XY and 46,XX disorders of sex development: bioinformatics consideration. Hum Mol Genet 2019; 28:2319-2329. .

27. Rossetti LZ, Glinton K, Yuan B, Liu P, Pillai N, Mizerik E, Magoulas P, Rosenfeld JA, Karaviti L, Sutton VR, Lalani SR, Scott DA. Review of the phenotypic spectrum associated with haploinsufficiency of MYRF. Am J Med Genet A 2019; 179:1376-1382. .

28. Chang Y-F, Imam JS, Wilkinson MF. The nonsense-mediated decay RNA surveillance pathway. Annu Rev Biochem 2007; 76:51-74. .

29. Emery B, Agalliu D, Cahoy JD, Watkins TA, Dugas JC, Mulinyawe SB, Ibrahim A, Ligon KL, Rowitch DH, Barres BA. Myelin Gene Regulatory Factor Is a Critical Transcriptional Regulator Required for CNS Myelination. Cell 2009; 138:172-85. .

30. Levinson G, Gutman GA. Slipped-strand mispairing: a major mechanism for DNA sequence evolution. Mol Biol Evol 1987; 4:203-21. .

31. Li Z, Park Y, Marcotte EM. A Bacteriophage tailspike domain promotes self-cleavage of a human membrane-bound transcription factor, the myelin regulatory factor MYRF. PLoS Biol 2013; 11:e1001624-.

32. Bujalka H, Koenning M, Jackson S, Perreau VM, Pope B, Hay CM, Mitew S, Hill AF, Lu QR, Wegner M, Srinivasan R, Svaren J, Willingham M, Barres BA, Emery B. MYRF is a membrane-associated transcription factor that autoproteolytically cleaves to directly activate myelin genes. PLoS Biol 2013; 11:e1001625-.

33. Kim D, Choi J-O, Fan C, Shearer RS, Sharif M, Busch P, Park Y. Homo-trimerization is essential for the transcription factor function of Myrf for oligodendrocyte differentiation. Nucleic Acids Res 2017; 45:5112-25. .

34. Huang H, Teng P, Du J, Meng J, Hu X, Tang T, Zhang Z, Qi YB, Qiu M. Interactive Repression of MYRF Self-Cleavage and Activity in Oligodendrocyte Differentiation by TMEM98 Protein. J Neurosci 2018; 38:9829-39. .

35. Cross SH, Mckie L, Keighren M, West K, Thaung C, Davey T, Soares DC, Sanchez-Pulido L, Jackson IJ. Missense Mutations in the Human Nanophthalmos Gene TMEM98 Cause Retinal Defects in the Mouse. Invest Ophthalmol Vis Sci 2019; 60:2875-87. .

Articles are provided courtesy of Emory University and the Zhongshan Ophthalmic Center, Sun Yat-sen University, P.R. China. The print version of this article was created on 21 September 2019. This reflects all typographical corrections and errata to the article through that date. Details of any changes may be found in the online version of the article.